Superconductor Science and Technology

Resistive broadening in sulfur doped FeTe

To cite this article: Swati Pandya *et al* 2010 *Supercond. Sci. Technol.* **23** 075015

IOP Publishing SUPERCONDUCTOR SCIENCE AND TECHNOLOGY
Supercond. Sci. Technol. **23** (2010) 075015 (6pp) doi:10.1088/0953-2048/23/7/075015

Resistive broadening in sulfur doped FeTe

Swati Pandya[1], **Siya Sherif**[1,2], **L S Sharath Chandra**[1,3] **and V Ganesan**[1]

[1] UGC-DAE Consortium for Scientific Research, University Campus, Khandwa Road, Indore (MP) 452017, India
[2] Department of Studies in Physics, University of Mysore, Manasagangothri, Mysore-570 006, India

Received 5 April 2010, in final form 7 May 2010
Published 16 June 2010
Online at stacks.iop.org/SUST/23/075015

Abstract
An analysis of resistive broadening in the presence of magnetic fields up to 14 T for sulfur doped FeTe superconductors is presented. FeTe shows an abrupt change in resistivity at 70 K due to a structural transition. Vanishing of the structural transition and the appearance of superconductivity at ∼10 K and 9.7 K are seen in $FeTe_{0.9}S_{0.1}$ and $FeTe_{0.8}S_{0.2}$ respectively. The upper critical field and coherence lengths are estimated using the Werthamer–Helfand–Hohenberg and Ginzburg–Landau theories for different criteria for the transition temperatures. The estimated activation energy for thermally activated flux flow (TAFF) is an order of magnitude smaller than for the rare earth (R) based $RFeAsO_{1-x}F_x$ system, which indicates weaker pinning than for the $RFeAsO_{1-x}F_x$ system. The flux flow activation energy shows power law behavior with the two different exponents for fields above and below $H = 6$ T for $FeTe_{0.9}S_{0.1}$ and $H = 8$ T for $FeTe_{0.8}S_{0.2}$. The fluctuation conductivity is analyzed using Aslamazov–Larkin theory and lowest Landau level (LLL) theory, respectively, for zero and nonzero magnetic fields. Incidentally, the field above which 2D LLL scaling is observed in these systems coincides with the crossover field observed in TAFF resistivity.

(Some figures in this article are in colour only in the electronic version)

1. Introduction

Recently, superconductivity has been reported in the iron chalcogenides FeSe and FeTe, and related systems. These systems are isostructural with the FeAs layer found in the iron arsenide superconductors [1–8]. Superconductivity in Fe compounds is quite interesting because generally, iron in many compounds has magnetic moments and they normally form an ordered magnetic state [1]. The superconducting transition temperature in FeSe has been increased from an initial 8 K to 14 K with appropriate Te substitution, and 36.7 K for the high pressure 8.9 GPa [1–10]. Tetragonal FeTe does not show a superconducting transition. However, it shows a tetragonal to orthorhombic structural transition along with long range SDW type antiferromagnetic order when the temperature is decreased below 80 K [2–8]. Density functional calculation indicates that the stability of the spin density wave is greater for FeTe than for FeSe, and hence, the doped FeTe achieves a higher T_C than FeSe [9, 10]. The suppression of the structural phase transition by the application of pressure induces superconductivity in other iron based systems [11–13]. For FeTe, the application of pressure up to 1.6 GPa shifts the structural transition to lower temperatures [6, 7]. However, superconductivity was not observed down to 2 K [6, 7]. Hence, it is believed that FeTe has the potential to produce superconductivity if an appropriate element is substituted to induce chemical pressure [6, 7]. Recently, superconductivity of $FeTe_{1-x}S_x$ was reported by Mizuguchi *et al* [6] with $T_C \sim$ 10 K for $x = 0.2$. Sulfur has the same number of valence electrons as Te and has a smaller ionic radius as compared to Te. Therefore, it is natural to expect the S substitution to induce positive chemical pressure on FeTe [7]. Since $FeTe_{1-x}S_x$ is composed of nontoxic elements, this material will be a good candidate for application [6]. The superconducting transition in $FeTe_{1-x}S_x$ is quite broad. Thermally activated flux flow (TAFF) and thermal fluctuation effects are two important reasons for the broadening of the superconducting transition. Hence, investigations of TAFF and fluctuation effects in $FeTe_{1-x}S_x$ may offer several hints as regards the potential for applications.

In the present work, we have investigated magneto-transport properties of FeTe, $FeTe_{0.9}S_{0.1}$ and $FeTe_{0.8}S_{0.2}$ in

[3] Present address: Materials, Advanced Accelerator Science Division, Raja Ramanna Centre for Advanced Technology, Indore-452 013, India.

magnetic field up to 14 T. The upper critical field $H_{C2}(0)$ and coherence lengths ξ are estimated using the Werthamer–Helfand–Hohenberg (WHH) and Ginzburg–Landau (GL) theories for $FeTe_{0.9}S_{0.1}$ and $FeTe_{0.8}S_{0.2}$. Resistive broadening of superconducting transitions is analyzed in terms of TAFF and thermal fluctuations. The activation energy for flow of vortices and its field dependent power law behavior are investigated. The fluctuation conductivity is analyzed for both superconductors using Aslamazov–Larkin (AL) theory and lowest Landau level (LLL) scaling, respectively, in zero and nonzero magnetic fields in order to understand the intrinsic superconducting characteristics and dimensionality of the system.

2. Experimental details

Polycrystalline FeTe, $FeTe_{0.9}S_{0.1}$ and $FeTe_{0.8}S_{0.2}$ samples were prepared using a solid state reaction method. The appropriate mixtures of Fe, Te and TeS were weighed and sealed in a quartz tube in the presence of a partial helium atmosphere and kept in the furnace for one day at 700 °C. The samples obtained were reground and pressed into pellets. The pellets were sealed into an evacuated quartz tube in the presence of a partial helium atmosphere and then heated to 700 °C and kept at that temperature for one day. The same procedure was repeated a second time. The samples were characterized by means of x-ray diffraction using Cu Kα radiation in a Rigaku diffractometer. Resistivity measurements were carried out using a Quantum Design Physical Property Measurement System (PPMS) down to 2 K and up to 14 T with a conventional four-probe method.

3. Results and discussion

The Rietveld refinement of the XRD reveals that all of the samples crystallize in tetragonal structure with the $P4/nmm$ space group at room temperature. The substitution of S in FeTe reduces the lattice parameters, indicating positive chemical pressure. The resistivities in the presence of a magnetic field for the FeTe, $FeTe_{0.9}S_{0.1}$ and $FeTe_{0.8}S_{0.2}$ are shown in figure 1. The resistivity of FeTe shows semiconducting behavior in the temperature range 80–300 K. Around $T_S \sim 70$ K there is a drop in resistivity due to the tetragonal to orthorhombic structural transition and this shows metallic behavior below T_S, but superconductivity is not observed in our measurement temperature range. A noticeable change in resistivity is not seen with the application of 14 T. The resistivity for $FeTe_{0.9}S_{0.1}$ and $FeTe_{0.8}S_{0.2}$ shows a semiconducting like to metallic crossover at around ∼35–40 K and shows the onset of superconductivity at ∼10 K and 9.7 K respectively. The transition is not sharp as in the case of conventional superconductors. The mean field T_C obtained from $d\rho/dT$ is 8.5 K and 8.1 K for $FeTe_{0.9}S_{0.1}$ and $FeTe_{0.8}S_{0.2}$ respectively.

The temperature dependent critical field H_{C2} is determined from $10\%\rho_n$, $50\%\rho_n$ and $90\%\rho_n$ criteria, and shown in figure 2. The values of dH_{C2}/dT for $10\%\rho_n$, $50\%\rho_n$ and $90\%\rho_n$ are −6.36, −6.85 and −7.99 T/K for $FeTe_{0.9}S_{0.1}$ and −6.38, −7.29, and −8.39 T/K for $FeTe_{0.8}S_{0.2}$ respectively.

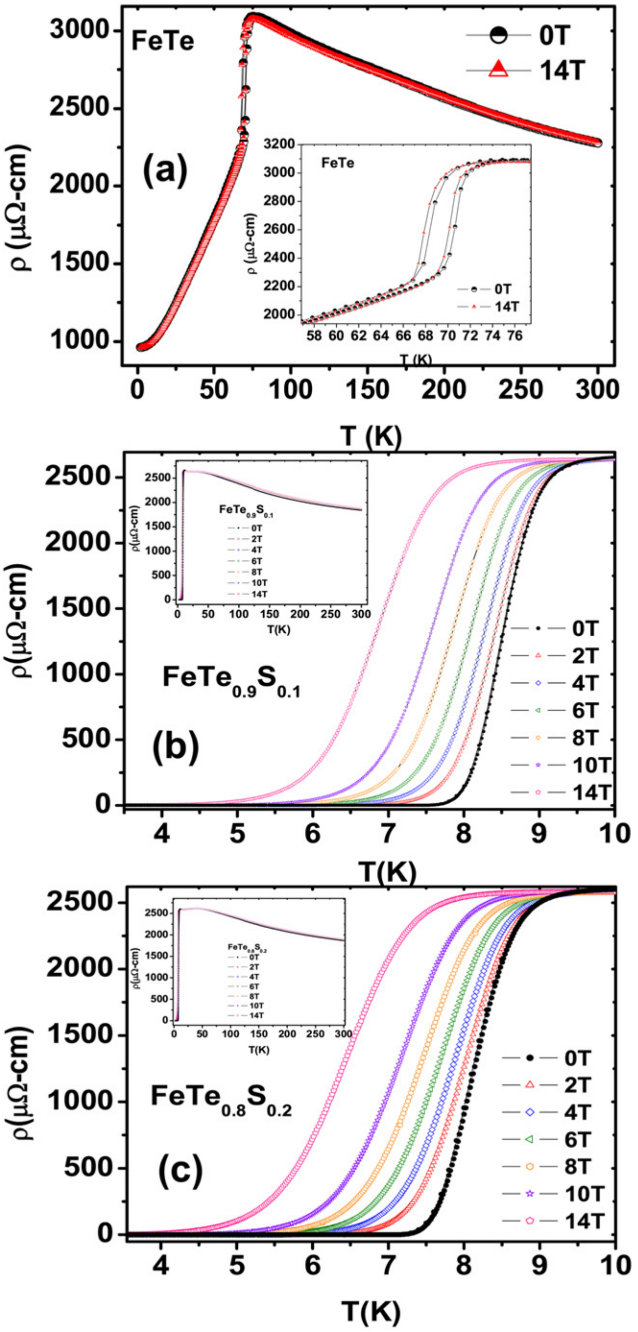

Figure 1. (a) Resistivity of FeTe in zero field and in the presence of 14 T. The inset shows hysteresis near the structural transition. The resistivities near T_C in the presence of a field up to 14 T for $FeTe_{0.9}S_{0.1}$ and $FeTe_{0.8}S_{0.2}$ are shown in (b) and (c) respectively. The insets show the resistivity in the temperature range 2–300 K in different fields.

According to the Werthamer–Helfand–Hohenberg (WHH) theory [14, 15], $H_{C2}^{WHH}(0)$ is given by $0.693\, T_C\, (dH_{C2}/dT)_{T_c}$. The $H_{C2}^{WHH}(0)$ estimated for $10\%\rho_n$, $50\%\rho_n$ and $90\%\rho_n$ are about 35, 40 and 50 T for $FeTe_{0.9}S_{0.1}$ and about 34, 44, and 51 T for $FeTe_{0.8}S_{0.2}$ respectively. The linear extrapolation of the H–T plot to $T = 0$ K for $90\%\rho_n$ results in values of $H_{C2}(0)$ of about 76 T for both samples.

One can calculate ξ along the ab plane for a polycrystalline sample from $90\%\rho_n H_{C2}(0)$, using GL theory,

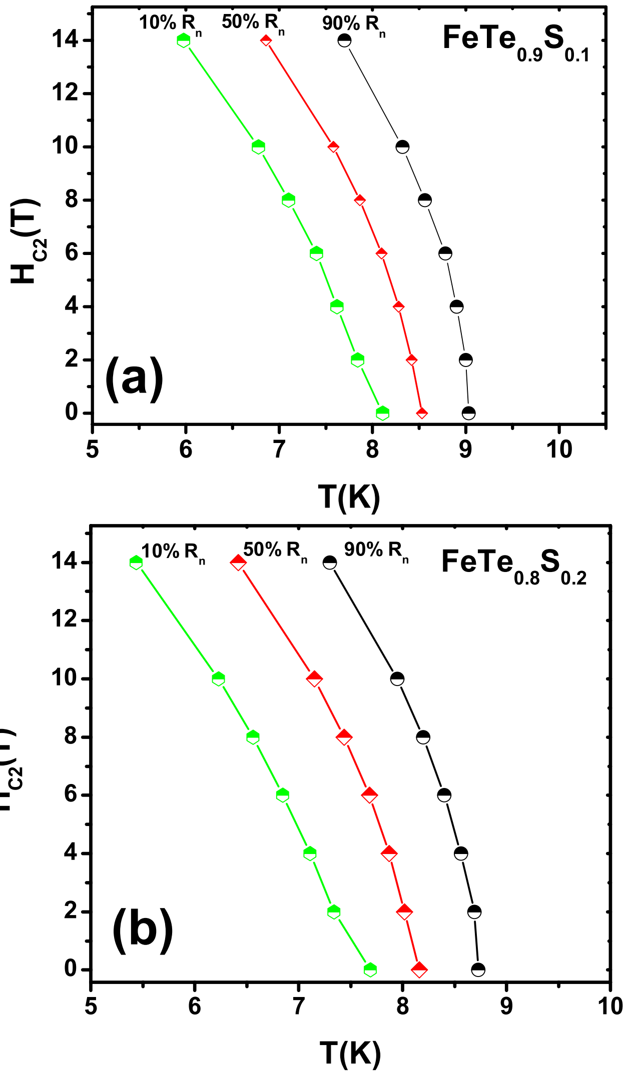

Figure 2. Upper critical fields H_{C2} versus T as determined from the 90%, 50% and 10% criteria of the normal state resistivity for (a) $FeTe_{0.9}S_{0.1}$ and (b) $FeTe_{0.8}S_{0.2}$.

as $\xi^2 = \varphi_0/2\pi\ H_{C2}$ [15–17]. The estimated ξ_{ab} is about 21–26 Å. The ξ_c is estimated from the conductivity fluctuations in zero magnetic field over a narrow region, where the 3D fluctuations are expected. The 3D fluctuations in the AL model can be expressed as $\Delta\sigma = A\varepsilon^{-0.5}$, where $\Delta\sigma$ is the excess conductivity, ε is $\ln(T/T_C)$, A is the temperature independent amplitude given by $A = e^2/32\hbar\xi_c(0)\sigma_0$ where σ_0 is the normal state conductivity just above the onset of the superconducting transition [18, 19]. The value of ξ_c turns out to be ~1 Å. If we use $\xi_{ab} \sim$ 21–26 Å and $\xi_c \sim 1$ Å, then the anisotropy factor $\gamma = \xi_{ab}/\xi_c \sim 20$ turns out to be approximately three times higher than the anisotropy factor ~5–9 of the $SmFeAsO_{1-x}F_x$ compound as reported in [16] and [20]. It is to be noted that values of $\gamma \sim 30$ were also reported using far-infrared ellipsometric measurements [21]. The values of ξ_{ab} obtained for our doped FeTe systems are quite comparable to those for the $RFeAsO_{1-x}F_x$ system [16]. The discrepancy appears to lie with ξ_c, which may be underestimated. This is because of the fact that ξ_c is estimated from the magnetization in [16] and [20], while in our case, ξ_c is estimated from resistivity data using fluctuation analysis. It is well known for superconductors that the parameters estimated from magnetization differ by orders of magnitude from those estimated from transport properties. The value of $\xi_c \sim 1$ Å, when compared to the interplanar spacing along the c-axis which is ~6 Å, indicates the 2D nature of the superconductivity.

The width of the superconducting transition in zero magnetic field is ~2.5 K and ~2.7 K for $FeTe_{0.9}S_{0.1}$ and $FeTe_{0.8}S_{0.2}$ respectively. Application of a magnetic field shifts the transition to lower temperature and makes it broaden further. The width of the transition observed at 14 T is 5 K for $FeTe_{0.9}S_{0.1}$ and 6 K for $FeTe_{0.8}S_{0.2}$. These numbers are quite large as compared to the zero-field distribution of T_C, which implies a significant role of vortex motion and the thermodynamic fluctuations.

The broadening of the superconducting transition in the presence of a magnetic field can be understood in terms of the activated flow of the vortices and described by the following Arrhenius law [15, 22–24]:

$$\rho(T, H) = \rho_0 \exp[-U_0/K_B T]$$

where U_0 is the activation energy for TAFF, K_B is the Boltzmann constant and ρ_0 is the pre-exponential factor. Figures 3(a) and (b) show the Arrhenius plot for both the superconductors in different magnetic fields. The slope of the Arrhenius plots for different magnetic fields extrapolates to a common point (T_m, ρ_0). All Arrhenius plots of figures 3(a) and (b) merge if the temperature scale is normalized to the form of $U_0(1/T - 1/T_m)$, as shown in the insets of figures 3(a)(i) and (b)(i) respectively; these findings are similar to our earlier results for $PrFeAsO_{0.6}F_{0.12}$ [15]. Here T_m is the only adjustable parameter and that too is limited by the experimental uncertainty. The insets in figures 3(a)(ii) and (b)(ii) show the magnetic field dependence of the activation energy (U_0/K_B). The activation energy is 203 K, 172 K in the lowest field 2 T and 73 K, 57 K for the highest field 14 T for $FeTe_{0.9}S_{0.1}$ and $FeTe_{0.8}S_{0.2}$ respectively. The activation energy is one order of magnitude smaller than that reported for $PrFeAsO_{0.6}F_{0.12}$ and $NdFeAsO_{0.7}F_{0.3}$ compounds [15, 24], which indicates weaker flux pinning for this system. The activation energy follows a power law behavior as $U_0/K_B \alpha H^{-n}$ with exponent $n \sim$ 0.34 and 0.45 for magnetic fields $H < 6$ T and $H < 8$ T and $n \sim$ 0.75 and 0.84 for magnetic fields $H > 6$ T and $H > 8$ T for $FeTe_{0.9}S_{0.1}$ and $FeTe_{0.8}S_{0.2}$ respectively. The activation energy becomes strongly field dependent above the 6 and 8 T magnetic fields for $FeTe_{0.9}S_{0.1}$ and $FeTe_{0.8}S_{0.2}$ respectively, which appears to be due to crossover from flux creep to flux flow of vortices. Power law behavior with two such different exponents is also observed in $NdFeAsO_{0.7}F_{0.3}$, $PrFeAsO_{0.6}F_{0.12}$ and the high T_C cuprates [15, 22–24].

Moreover, the fluctuation conductivity also plays an important role in the broadening of the superconducting transition. The fluctuation effects are quantified by the Ginzburg number, which can be expressed for a 3D superconductor as $Gi_{3D} = (\pi k^2 \xi_0 K_B T_C \mu_0/2\varphi_0^2)^2$, where $K = \lambda_0/\xi_0$ is the GL parameter, λ_0 is the London penetration depth,

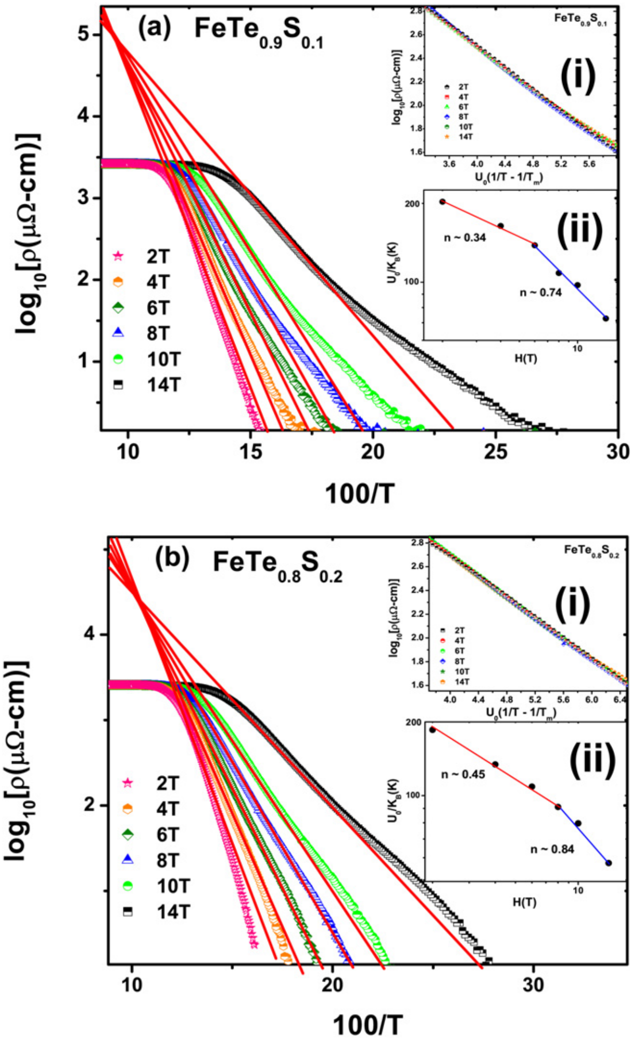

Figure 3. The Arrhenius plot of the resistivity in different fields for (a) $FeTe_{0.9}S_{0.1}$ and (b) $FeTe_{0.8}S_{0.2}$. The solid lines are linear fits to the data. The insets show log ρ versus $U_0(1/T - 1/T_m)$ and the field dependent activation energy (U_0) of the flux flow.

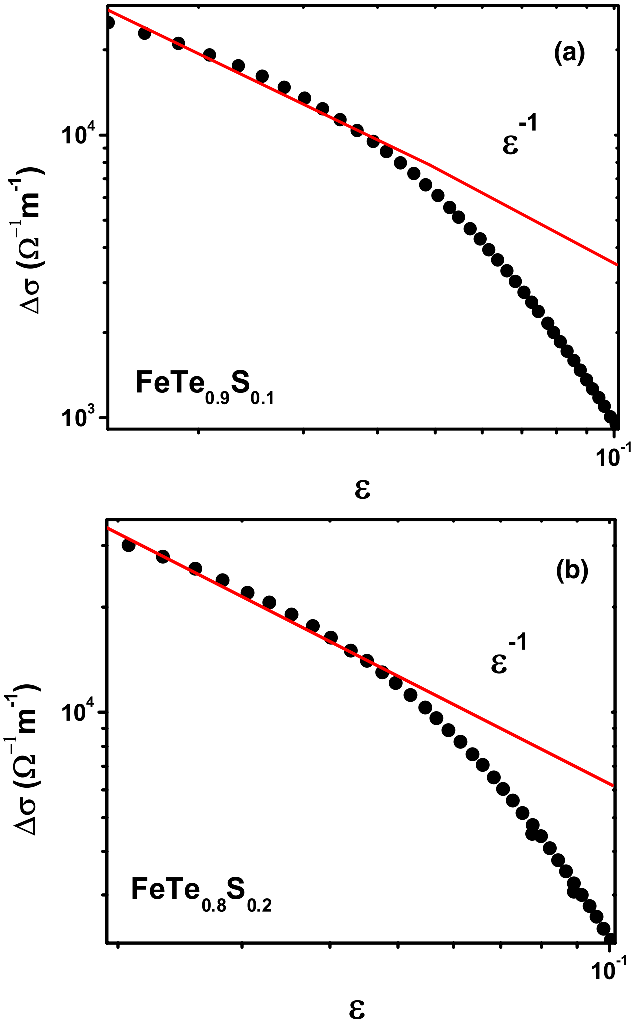

Figure 4. The variation of the normalized excess conductivity versus reduced temperature in a ln–ln plot for (a) $FeTe_{0.9}S_{0.1}$ and (b) $FeTe_{0.8}S_{0.2}$.

ξ_0 is the coherence length, K_B is the Boltzmann constant and φ_0 is the flux quantum [16, 17]. The Ginzburg number for a 2D superconductor is given as $Gi_{2D} = K_B T_C/E_F$, where E_F is the Fermi energy [16]. For the present system with $T_C \sim 8.5$ K, $\xi_0 \sim 0.5$ nm, which is calculated from $\xi_0 = (\xi_{ab}\xi_c)^{1/2}$, and assuming $\lambda \sim 405$ nm [25], we estimate $Gi_{3D} \sim 0.006$. This value is in good agreement with that for $SmFeAsO_{1-x}F_x$ [16]. We estimate $Gi_{2D} \sim 0.02$, by assuming $E_F \sim 35$ meV obtained from the thermoelectric power, which is not shown here—which is high as compared to that for $SmFeAsO_{1-x}F_x$ [16].

To probe the fluctuation dimensionality, the fluctuation conductivity in zero magnetic field due to finite Cooper pair formation above T_C is analyzed in the light of AL theory. As said earlier, according to AL theory, the fluctuation conductivity $\Delta\sigma$ is given by $A\varepsilon^{\alpha}$, where the conductivity exponent α varies from -0.3 to -3 for different dimensionalities of the conductivity fluctuations [18, 19]. We show $\Delta\sigma$ in zero magnetic field as a function of ε for both samples in figure 4. We have observed a 2D behavior $(\Delta\sigma)_{2D}\alpha\varepsilon^{-1}$ near the transition temperature, i.e. 8.6–8.9 K for $FeTe_{0.9}S_{0.1}$ and 8.2–8.5 K for $FeTe_{0.8}S_{0.2}$. The effective layer thickness (d) estimated using the equation $A = e^2/16hd\sigma_0$ [18, 19] is about 1 Å.

The superconducting fluctuations in the presence of a magnetic field are analyzed using the lowest Landau level (LLL) scaling. In a strong magnetic field the paired quasiparticles are effectively limited to being in their lowest Landau level; the superconducting fluctuations in bulk low T_C as well as in high T_C materials acquire an effective one-dimensional (1D) character along the field direction. This reduction of the effective dimensionality increases the importance of the fluctuations, resulting in a fluctuation region around $T_C(H)$ [16, 26]. Magnetic field induced fluctuation conductivity can be analyzed using the formalism developed by Ullah and Dorsey [16, 26–30]. Following the same analysis, the scaling laws for the 2D and 3D excess conductivity ($\Delta\sigma$) due to fluctuations in the magnetic fields are given by

$$\Delta\sigma(H)_{2D} = (T/H)^{1/2} F_{2D}(A[(T - T_c(H))/(TH)^{1/2}]) \quad (1)$$

$$\Delta\sigma(H)_{3D} = (T^2/H)^{1/3} F_{3D}(B[(T - T_c(H))/(TH)^{2/3}]) \quad (2)$$

where A and B are characteristic constants of the material.

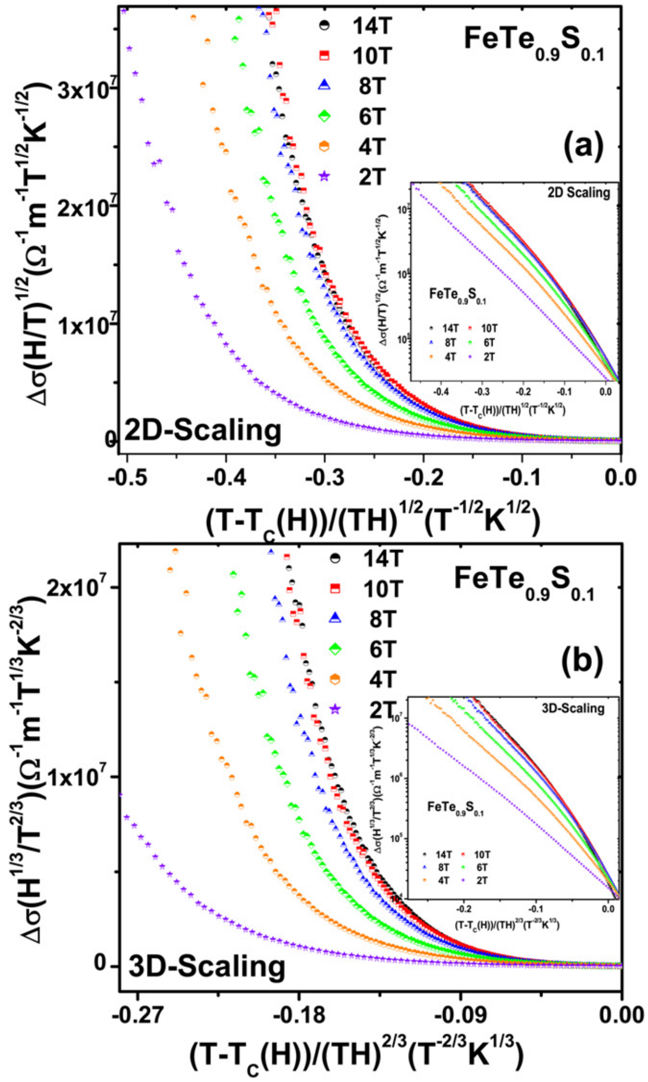

Figure 5. The lowest Landau level (a) 2D and (b) 3D scaling for $FeTe_{0.9}S_{0.1}$ for magnetic field up to 14 T. In the insets, the same plots are shown on a semilogarithmic scale.

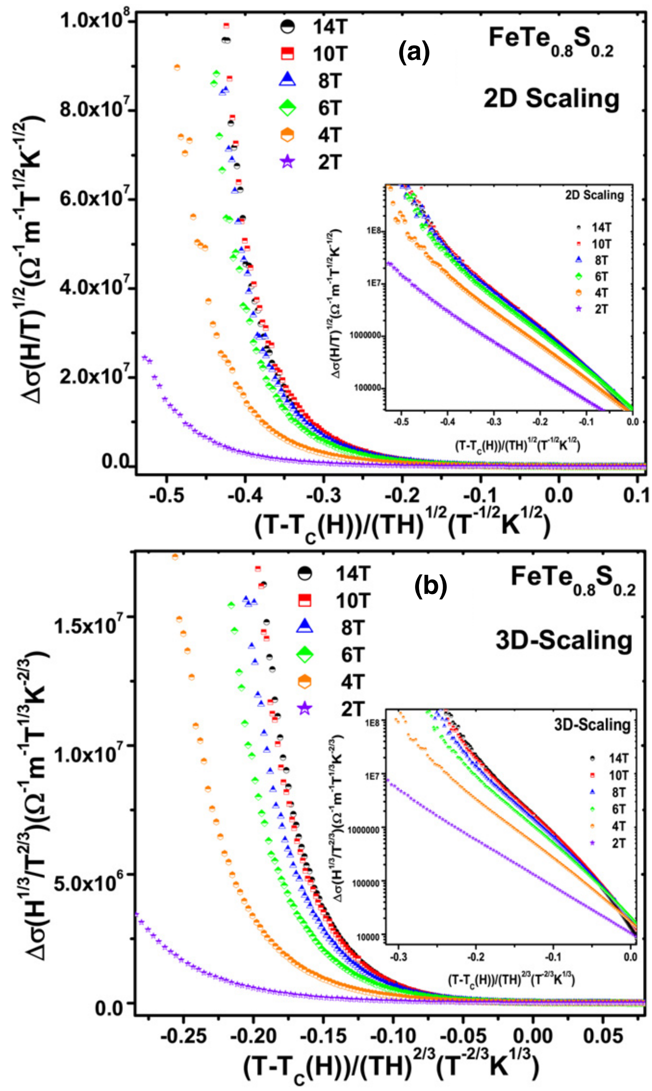

Figure 6. The lowest Landau level (a) 2D and (b) 3D scaling for $FeTe_{0.8}S_{0.2}$ for magnetic field up to 14 T. In the insets, the same plots are shown on a semilogarithmic scale.

Recently, 2D LLL scaling was observed for new $SmFeAsO_{1-x}F_x$ superconductor above $\mu_0 H_{\mathrm{LLL}} \sim 8$ T [16]. To verify the 2D nature of the fluctuations in our system, we have plotted $\Delta\sigma(H/T)^{1/2}$ versus $[(T - T_c(H))/(TH)^{1/2}]$ for 2D scaling and $\Delta\sigma(H^{1/3}/T^{2/3})$ versus $[(T - T_c(H))/(TH)^{2/3}]$ for 3D LLL scaling in figures 5 and 6. The same plots on a semilogarithmic scale are shown in the insets of figures 5 and 6. The x-axis for 2D and 3D scalings is chosen so that they correspond to the same temperature interval. The 2D relationship provides better scaling of data below and close to T_C above $\sim$8 T for $FeTe_{0.9}S_{0.1}$ and above $\sim$6 T for $FeTe_{0.8}S_{0.2}$. The scaling appears to be good in the 2D case, as compared to the 3D scaling, which is clearly seen on a semilogarithmic scale, indicating the 2D nature of the superconductivity.

4. Conclusion

In summary, 10% and 20% substitution of sulfur in FeTe leads to vanishing of the structural transition and induction of superconductivity. The upper critical field $H_{C2}(0)$ was estimated to be $\sim$50 and $\sim$51 T for $FeTe_{0.9}S_{0.1}$ and $FeTe_{0.8}S_{0.2}$ from WHH theory and $\sim$76 T from linear extrapolation to $T = 0$. The activation energy of the flux flow is one order of magnitude smaller than for the $RFeAsO_{1-x}F_x$ system, indicating weaker pinning than that for the $RFeAsO_{1-x}F_x$ system. The magnetic field dependent activated energy (U/K_0) shows power law behavior with two different exponents for regions above and below 6 T for $FeTe_{0.9}S_{0.1}$ and 8 T for $FeTe_{0.8}S_{0.2}$. The ab plane coherence length ξ_{ab} is calculated to be about 26–21 Å from the upper critical field. The out of plane coherence length ξ_c calculated from the zero-field excess conductivity due to fluctuations is about $\sim$1 Å, which is smaller than the interplanar spacing $\sim$6 Å, characterizing the 2D nature of the superconductivity. This result is further corroborated by (a) observation of the 2D nature of the fluctuations in zero magnetic field in a narrow temperature range around the transition, (b) the results for magnetic field induced fluctuation conductivity close to and below $T_C(H)$, which shows a clear 2D lowest Landau level scaling for fields above $\mu_0 H_{LLL} \sim 8$ T for $FeTe_{0.9}S_{0.1}$ and $\mu_0 H_{LLL} \sim 6$ T for $FeTe_{0.8}S_{0.2}$. Incidentally, the field range above which 2D LLL scaling is observed in these systems coincides with that for the crossover fields observed in TAFF related resistivity. This interesting coincidence warrants further investigation.

Acknowledgments

The authors thank Dr P Chaddah and Professor Ajay Gupta for their support and encouragement, Mr P Saravanan and Mr M Gangrade, staff of the low temperature and cryogenics laboratory, for their technical support and Ms Deepti Jain for her interest. We acknowledge the support of DST, India, for the LTHM Project, and DST and CSIR for a fellowship to SP. LSSC thanks Dr S B Roy, RRCAT, Indore, for his encouragement and BRNS for a KSKRA fellowship.

References

[1] Medvedev S *et al* 2009 *Nat. Mater.* **8** 630–3
[2] Hsu F C *et al* 2008 *Proc. Natl Acad. Sci. USA* **105** 14262
[3] Fang M H, Pham H M, Qian B, Liu T J, Vehstedt E K, Liu Y, Spinu L and Mao Z Q 2008 *Phys. Rev.* B **78** 224503
[4] Li S *et al* 2009 *Phys. Rev.* B **79** 054503
[5] Chen G F, Chen Z G, Dong J, Hu W Z, Li G, Zheng X D, Zheng P, Luo J L and Wang N L 2009 *Phys. Rev.* B **79** 140509
[6] Mizuguchi Y, Tomioka F, Tsuda S, Yamaguchi T and Takano Y 2009 *Appl. Phys. Lett.* **94** 012503
[7] Wu M K *et al* 2009 *Physica* C **469** 340
[8] Mizuguchi Y, Tomioka F and Tsuda S 2009 *J. Phys. Soc. Japan* **78** 074712
[9] Subedi A, Zhang L, Singh D J and Du M H 2008 *Phys. Rev.* B **78** 134514
[10] Zhang L, Singh D J and Du M H 2009 *Phys. Rev.* B **79** 012506
[11] Ishikawa F, Eguchi N, Kodama M, Fujimaki K, Einaga M, Ohamara A, Nakayama A, Mitsuda A and Yamada Y 2009 *Phys. Rev.* B **79** 172506
[12] Mani A, Ghosh N, Paulraj S, Bharathi A and Sunder C S 2009 *Europhys. Lett.* **87** 17004
[13] Takeshita N, Yamazaki T, Iyo A, Eisakim H, Kitom H, Ito T, Hirayama K, Fukazawa H and Kohori Y 2008 *J. Phys. Soc. Japan* **77** 131
[14] Werthamer N R, Helfand E and Hohenberg P C 1966 *Phys. Rev.* **147** 295
[15] Bhoi D, Sharath Chandra L S, Choudhury P, Ganesan V and Mandal P 2009 *Supercond. Sci. Technol.* **22** 095015
[16] Pallecchi I, Fanciulli C, Tropeano M, Palenzona A, Ferretti M, Malagoli A, Martinelli A, Sheikin I, Putti M and Ferdeghini C 2009 *Phys. Rev.* B **79** 104515
[17] Hunte F, Jaroszynski J, Gurevich A, Larbalestier D C, Jin R, Sefat A S, McGuire M A, Sales B C, Christen D K and Mandrus D 2008 *Nature* **453** 903
[18] Friedmann T A, Rice J P, Giapintzakis J and Ginsberg D M 1989 *Phys. Rev.* B **39** 4258
[19] Abou-Aly A I, Awad R, Ibrahim I H and Abdeen W 2009 *Solid State Commun.* **149** 281
[20] Balicas L *et al* 2009 arXiv:0809.4223
[21] Dubroka A, Kim K W, Rossle M, Malik V K, Drew A J, Liu R H, Wu G, Chen X H and Bernhard C 2008 *Phys. Rev. Lett.* **101** 097011
[22] Palstra T T M, Batlogg B, Van Dover R B, Schneemeyer L F and Waszczak J V 1989 *Phys. Rev.* B **41** 6621
[23] Wang X L *et al* 2005 *J. Appl. Phys.* **97** 10B114
[24] Jaroszynski J *et al* 2008 *Phys. Rev.* B **78** 174523
[25] Khasanov R *et al* 2008 *Phys. Rev.* B **78** 220510
[26] Welp U, Fleshler S, Kwok W K, Klemm R A, Vinokur V M, Downey J, Veal B and Crabtree G W 1991 *Phys. Rev. Lett.* **67** 22
[27] Kim D H, Gray K E and Trochet M D 1991 *Phys. Rev.* B **45** 10801
[28] Costa R M, Pureur P, Gusmao M, Senoussi S and Behnia K 2001 *Phys. Rev.* B **64** 214513
[29] Ullah S and Dorsey A T 1990 *Phys. Rev. Lett.* **65** 2066
[30] Ullah S and Dorsey A T 1991 *Phys. Rev.* B **44** 262